International Journal of Robotics and Control Systems
Vol. 5, No. 2, 2025, pp. 990-1005
ISSN 2775-2658
http://pubs2.ascee.org/index.php/ijrcs

Enhancement of Transient Stability and Power Quality in Grid-Connected PV Systems Using SMES

Samira Heroual [a,1], Belkacem Belabbas [a,2], I. M. Elzein [b,3], Yasser Diab [c,4], Alfian Ma'arif [d,5], Mohamed Metwally Mahmoud [e,6,*], Tayeb Allaoui [a,7], Naima Benabdallah [a,8]

[a] Department of Electrical Engineering, Laboratory of L2GEGI, Ibn Khaldoun University, Tiaret, Algeria
[b] Department of Electrical Engineering, College of Engineering and Technology, University of Doha for Science and Technology, Doha P.O. Box 24449, Qatar
[c] Nantes Université, Institut de Recherche en Énergie Électrique de Nantes Atlantique (IREENA, UR 4642), Saint-Nazaire, 44600, France
[d] Department of Electrical Engineering, Universitas Ahmad Dahlan, Yogyakarta, Indonesia
[e] Electrical Engineering Department, Faculty of Energy Engineering, Aswan University, Aswan 81528, Egypt.
[1] samira.heroual@univ-tiaret.dz; [2] Belabbas.belkacem@univ-tiaret.dz; [3] Yasser.Diab@univ-nantes.fr;
[4] 60101973@udst.edu.qa; [5] alfian.maarif@te.uad.ac.id; [6] metwally_m@aswu.edu.eg; [7] tayeb.allaoui@univ-tiaret.dz;
[8] naima.benabdallah@univ-tiaret.dz
* Corresponding Author

ARTICLE INFO

Article history
Received January 04, 2025
Revised March 20, 2025
Accepted April 09, 2025

Keywords
Grid-Connected PV Power;
SMES;
Power Quality;
DC Link Voltage;
Transient Stability

ABSTRACT

One of the main issues with grid-connected distributed energy systems, including photovoltaic (PV) systems, is the DC bus voltage's instability during load fluctuations and power line short circuits. This paper attempts to address this problem and proposes to use superconducting magnetic energy storage (SMES) to stabilize the voltage of the DC link and improve the power quality and transient stability of the power system. The investigated configuration components are PV cells, boost converter, chopper, SMES, three level inverter (NPC), filter, grid, and load. MATLAB / Sim Power System is used to test the performance of a SMES in order to ensure the balance of the DC bus voltage of a PV system connected to the grid. Several scenarios were considered to show the performance and benefits of combining a SMES with the PV system. The outcomes of the examined scenarios (fault and load change) demonstrate the precision of the employed control systems, maintaining the DC voltage at acceptable levels (≈500 V), enhances the structure stability, and improving power quality (GPV THD = 4.34). Finally, it can be concluded that the proposed configuration will help in achieving high penetration scenarios of PV systems.

1. Introduction

In recent years, with the increasing deployment of Renewable Energy Sources (RES) such as Photovoltaic (PV) energy into the grid, the quality electrical supply has become vitally important for utility providers, electrical power industry and consumers. Hence, there has been a growing interest in the design of new methods and devices to address power quality (PQ) issues and improve the efficiency and reliability of the distribution grid [1]-[5]. Several authors have studied the integration of PV systems into the grid, but the main problems encountered are the quality of energy produced and the instability of the DC bus to short circuit defects and load variation [6]-[11] .

After studies in [12]-[16] multilevel inverters, especially the Neutral-Point-Clamped (NPC) topology, have become very popular power converters in PV energy applications with high-power [17]-[20]. It presents many advantages when compared with the classical two-level converter such as reducing the Total Harmonic Distortion (THD) and improving output voltage waveform. However, the main disadvantage of these types of converters is the instability of the capacitor voltage in the intermediate circuit.

According to the bibliographical research, to solve this problem two algorithms control is proposed is consist of two loops. The outer closed-loop controls the average value of the DC voltage using a PI regulator, whereas the inner loop controls the difference between the two voltages in each half-arm using a clamping bridge circuit [21], [22]. In this paper, we used the five-level NPC inverter. Another important element that plays a major role in the PV system is the Energy Storage System (ESS) [23]. In this paper, a high-power storage system SMES type is characterized by a fast dynamic to discharge the energy to the load and it is a long life compared to small ESS such as batteries [24]-[27].

The amount of power that can be captured from a PV system depends on several parameters including the temperature and illumination. The Maximum Power Point Tracking (MPPT) algorithms are designed to search for the optimum operating point that allows the PV system to extract the maximum power from the available PV energy [28]. Various optimal power monitoring control strategies were already discussed in the literature for obtaining better energy conversion efficiency for all meteorological data, such as the Perturb and Observe (P&O) algorithm and incremental conductance are most commonly used in MPPT algorithms [29]-[32]. These control strategies have some disadvantages such as robustness, complexity, and difficulty for implementation. To overcome these disadvantages and ensure the MPPT efficiency of a PV system, several types of research as part of the artificial intelligence approach [33], [34] and robust nonlinear controller to achieve the conversion efficiency of the maximum energy of a PV system [35]. Robust nonlinear controllers based on Lyapunov stability have been proposed in the literature to improve PV performance under difficult operating conditions. Among these, Sliding Mode Controller (SMC) has been extensively applied because of its insensitivity to variations in internal and external parameters, its stability, its simplicity of implementation, and fast response. However, the main disadvantage of this control strategy is the presence of a chattering phenomenon. To eliminate this problem a Super-Twisting SMC (STSMC) is employed in this paper for the MPPT algorithm [36]. To strengthen the introduction and provide a stronger rationale for the proposed methodology, Table 1 is presented.

Table 1. Contrasting the present work with the most well-known research in the field

Ref.	Year	Publisher	System components	Bus type	Controller	Case studies
[37]	2021	IEEE	WT, SMES, and battery	DC	PI	Wind fluctuations (WFs)
[38]	2021	Elsevier	PV, SMES, and battery	AC	PI and FLC	Load change (LC)
[39]	2020	IEEE	WT, SMES, and battery	AC	PI	WFs
[40]	2018	ICPES	WT, supercapacitor, and battery	DC	PI	WFs
[41]	2018	ICEES	PV, , supercapacitor, and battery	DC	Rule based controller	Variable irradiance (VI), and LC
[42]	2018	IEECON	PV, WT, supercapacitor, and battery	DC	Ramp rate limiter	LC
[43]	2023	MDPI	PV, Biogas with Pumped-Hydro Storage system, and SMES	AC	Optimized controller	LC, and VI
Current work			PV	DC	STSMC	LC, and three phase fault

The contribution of this article is to add a storage system connected to the DC bus using a four-quadrant chopper for the purpose of ensuring the stability of the DC voltage against the load variation and the short circuit fault. STSMC is employed for MPPT. Improving the quality of energy produced

by the PV system with the application of a five-level inverter where it can reduce swithching losses and THD percentage and to ensure the stability of the DC voltage by using the SMES.

The rest of the paper is organized as follows: Section 2 presents a description and modeling of the PV/SMES system connected to the grid. The control strategies are presented in Section 3. Finally, simulation results and conclusions are presented in Section 4 and Section 5, respectively.

2. Modeling of Grid-Connected PV-SMES System

The proposed grid-connected PV-SMES system is shown in Fig. 1. The way the components of the system under investigation are modeled and integrated into the overall system. The PV array is connected to the DC bus via a boost converter controlled by a MPPT algorithm to extract the maximum power. The DC bus is then connected to the AC bus through the NPC three-level inverter. The SMES is connected to the DC via DC chopper.

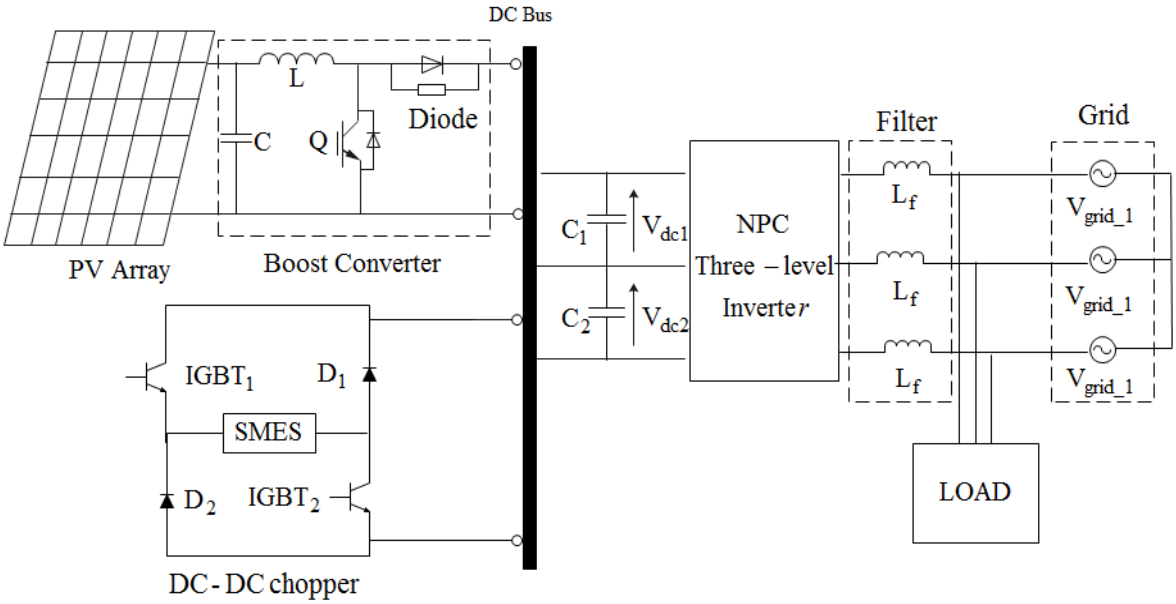

Fig. 1. Proposed grid-connected PV-SMES system

2.1. PV Array

A basic equivalent circuit model of a PV cell is depicted in Fig. 2. The modeling of this solar cell is well presented in [44]-[47].

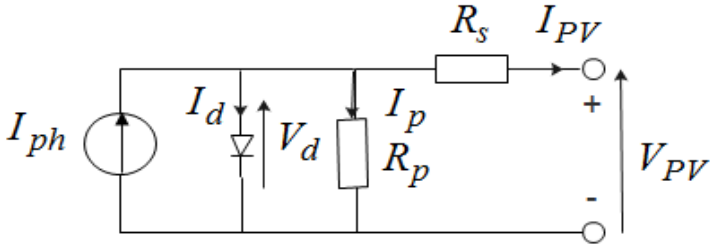

Fig. 2. PV cell circuit model

2.2. Three-Level NPC Inverter

The topology of the three-level NPC converter shown in Fig. 3. It consists of two series capacitors (C_1, C_2) forming a midpoint noted (0) which allows the converter to access an additional voltage level compared to the conventional converter. at two levels.

This structure consists of three arms $(1, 2, 3)$, each of the three arms is composed of four controlled switches $(T_{11}, T_{12}, T_{13}, T_{14})$ and two clamp diodes (DD_{11}, DD_{10}) (for the arm (1).

connected to the midpoint of the DC bus are used to clamper the terminal of each controlled switch to the midpoint of the DC bus. The controlled switches must be bidirectional in current and unidirectional in voltage, they are associations of a transistor and a diode in antiparallel. The modeling of three-level NPC converter is discussed in more detail in [22].

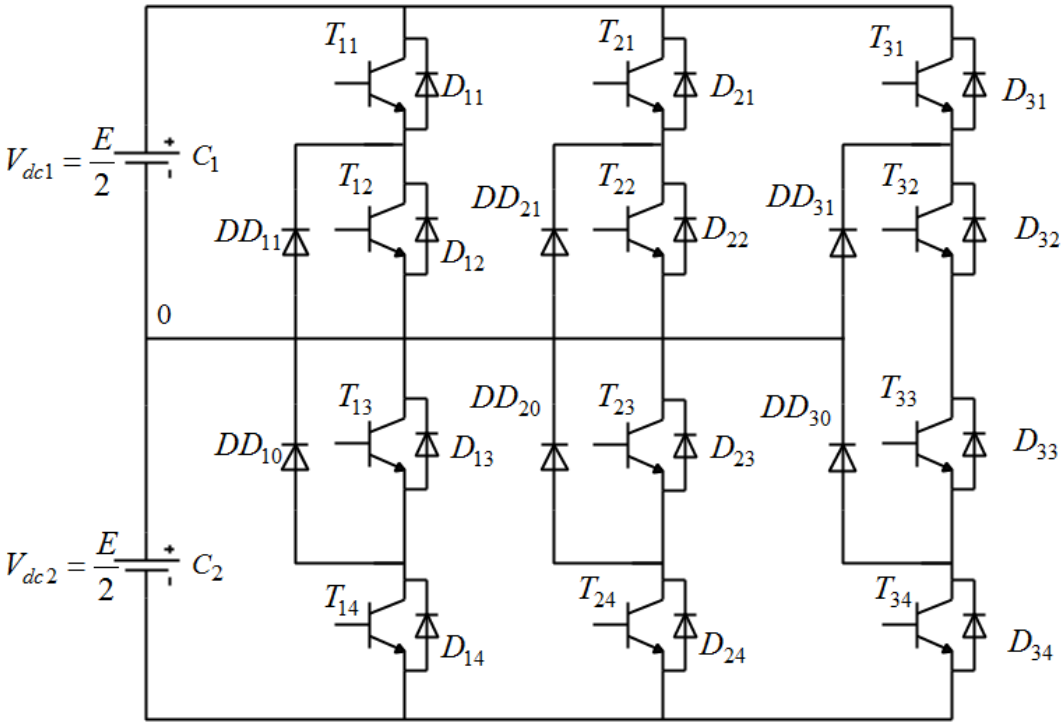

Fig. 3. Topology of the three-level NPC inverter

2.3. Modeling of Intermediate Filter

The clamping bridge consists of a transistor in series with a resistance, inserted to improve and stabilize the DC-voltage dynamic [48]. The intermediate filter scheme with clamping bridge seen in Fig. 4.

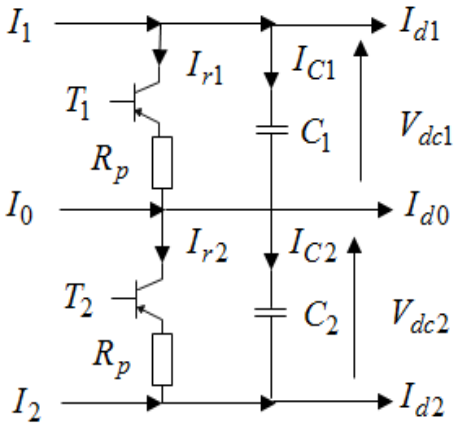

Fig. 4. Intermediate filter structure with clamping bridge

The mathematical model of the intermediate filter given by:

$$\begin{cases} C_1 \dfrac{dV_{dc1}}{dt} = I_1 - I_{r1} - I_{d1} \\ C_2 \dfrac{dV_{dc2}}{dt} = -I_2 - I_{r2} - I_{d2} \end{cases} \quad (1)$$

With

$$\begin{cases} I_{r1} = \dfrac{V_{dc1}}{R_P} \\ I_{r2} = \dfrac{V_{dc2}}{R_P} \end{cases} \tag{2}$$

2.4. Modeling of Intermediate Filter

The SMES is a superconducting coil where energy is stored in the form of a magnetic field generated by the current flowing in the coil. The SMES is known for its high-power density and high speed of charge and discharge which makes it suitable for PV systems. The stored energy of SMES can be expressed as [49], [50]:

$$W_{sm} = W_{sm0} + \int_{t_0}^{t} P_{sm}\, d\tau \tag{3}$$

$$W_{sm0} = \frac{1}{2} L_{sm} I_{sm0}^2 \tag{4}$$

$$P_{sm} = \frac{dW_{sm}}{dt} = L_{sm} I_{sm}.W_{sm0} \frac{dI_{sm}}{dt} = I_{sm} V_{sm} \tag{5}$$

The modelling of SMES is discussed in more details in [51].

3. Control Strategies

This section provides a detailed description and design steps of the different control strategies for PV system.

3.1. Nonlinear STSMC Control Design for MPPT Algorithm

In this section, the basic principle and the design procedure of the MPPT algorithm based of STSMC are presented. The STSMC has the ability to eliminate chattering, which is inherent in conventional SMC (Sliding Mode Control). In addition, it retains the same tracking and robustness performance of the conventional SMC [52]. The STSMC scheme consists of two terms: the equivalent control U_{equ} and super twisting control U_{st}.

$$u(t) = u_{equ}(t) + u_{st}(t) \tag{6}$$

$$u_{st}(t) = u_1(t) + u_2(t) \tag{7}$$

$$\begin{cases} u_1(t) = -\lambda.|S|^{1/2}.sgn\,(S) \\ u_2(t) = -\int \gamma.sgn(S)\ \ dt \end{cases} \tag{8}$$

where λ and γ are the positive constants and the fixed-gain can choose as:

For the equivalent control of STSMC, the same procedure is used as for the conventional SMC. Its design procedure applied for a MPPT algorithm include the following steps:

(A) Equivalent control

The switching surface is designed as:

$$S = \frac{\partial P_{PV}}{\partial V_{PV}} = \frac{\partial (V_{PV}.I_{PV})}{\partial V_{PV}} \tag{9}$$

$$S = I_{PV} + V_{PV}\frac{\partial I_{PV}}{\partial V_{PV}} \tag{10}$$

$$S = V_{PV}\left(\frac{\partial I_{PV}}{\partial V_{PV}} + \frac{I_{PV}}{V_{PV}}\right) \tag{11}$$

$$S = V_{PV}\left(\frac{I_{PV}(k) - I_{PV}(k-1)}{V_{PV}(k) - V_{PV}(k-1)} + \frac{I_{PV}(k)}{V_{PV}(k)}\right) \tag{12}$$

The PV output power is controlled by adjusting the duty cycle α of the boost converter. Thus, the equivalent control given by:

$$U_{equ}(t) = \alpha = 1 - \frac{V_{in}}{V_o} \tag{13}$$

(B) Super-Twisting Control (STC)

In this work, the hyperbolic tangent surface is used for the STC due to its robustness and fast convergence. For the STC terms can written as [53], [54]:

$$U_{st}(t) = -\lambda.|S|^{1/2}.tanh\,(S) - \int \gamma.tanh(S).dt \tag{14}$$

The positive gains for λ and γ are chosen to fulfil the condition of convergence.

3.2. Clamping Bridge Control

The control algorithm, which controls the clamping bridge, applied separately for the upper and the lower stages. The algorithm compares, in real-time, the differences (ΔV_{12}) in the DC voltages of each stage to zero. If the difference is not equal to zero, the excess of energy will be dissipated through the resistance. The control algorithm of the clamping bridge given as follows [51]-[56]:

$$\begin{cases} \Delta V_{12} > 0 \Rightarrow I_{r1} = 0 \& I_{r2} \neq 0 (T_1 = 0 \& T_2 = 1) \\ \Delta V_{12} > 0 \Rightarrow I_{r1} \neq 0 \& I_{r2} = 0 (T_1 = 1 \& T_2 = 0) \end{cases} \tag{15}$$

$$Avec: \Delta V_{12} = V_{dc1} - V_{dc2} \tag{16}$$

3.3. Control the DC Chopper

Fig. 5 shows the configuration of the DC chopper connected to the SMES device. The circuit operates in charging or discharging modes by adjusting the duty cycle of the chopper to regulate the DC bus voltage in response to various operating conditions of the PV system [57], [43], [58], [59]. The goal in controlling the SMES current is to control the required power.

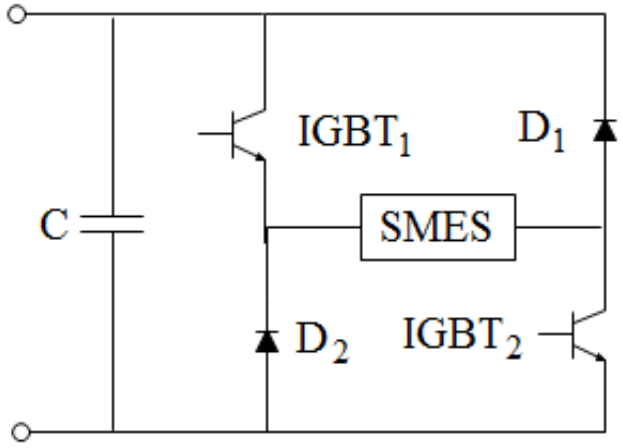

Fig. 5. Configuration of the DC chopper

In steady-state, the DC voltage and the SMES voltage are related as follows:

$$V_{dc} = \left(\frac{D}{1-D}\right).V_{sm} \tag{17}$$

There are three modes of operation for the SMES: the state of charge, state of expectation and the discharge state. Fig. 6 shows the operation of the DC chopper in these three modes. When SMES is charging (discharging), the D is more than 0.5 (D is less than 0.5) is on and the converter operates in boost (buck) mode. Furthermore, if the D is 0 the DC-DC chopper operation will be in standby mode.

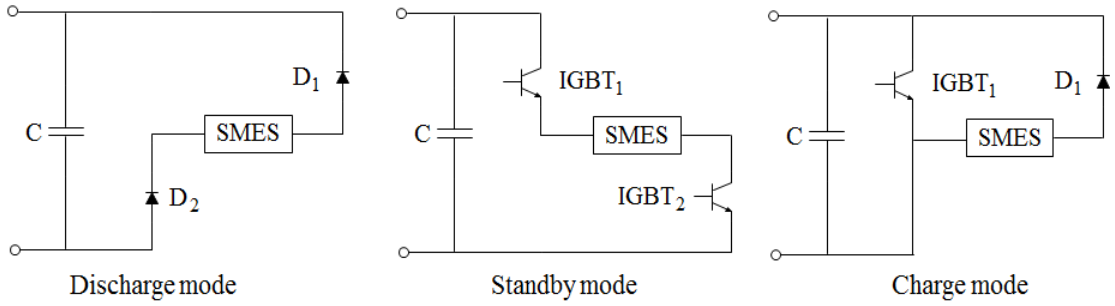

Fig. 6. Operating modes of the DC chopper

3.4. Control of the Injected Powers

There are several strategies for controlling active and reactive power (P, and Q), among which the instantaneous power method is generally used in production systems to control the P, and Q injected into the power grid [22], [60]. The P, and Q in the Concordia coordinate system are expressed by the following two equations:

$$\begin{cases} P = \frac{3}{2}(V_\alpha I_\alpha + V_\beta I_\beta) \\ Q = \frac{3}{2}(V_\beta I_\alpha - V_\alpha I_\beta) \end{cases} \tag{18}$$

The reference currents are calculated according to the following equation system:

$$\begin{cases} i_a^* = \frac{2}{3}\left(\frac{P.V_\alpha + Q.V_\beta}{V_\alpha^2 + V_\beta^2}\right) \\ i_\beta^* = \frac{2}{3}\left(\frac{P.V_\beta - Q.V_\alpha}{V_\alpha^2 + V_\beta^2}\right) \end{cases} \tag{19}$$

By injecting only, the P generated by the PV generator for the purpose of ensuring a unit power factor. It is imposed that the Q injected is equal to zero ($Q^* = 0$). Equation (18) becomes:

$$\begin{cases} i_a^* = \frac{2}{3}\left(\frac{P.V_\alpha}{V_\alpha^2 + V_\beta^2}\right) \\ i_\beta^* = \frac{2}{3}\left(\frac{P.V_\beta}{V_\alpha^2 + V_\beta^2}\right) \end{cases} \tag{20}$$

The power control scheme is seen in Fig. 7. The PWM technique is used to control the 3-level inverter.

4. Simulation Results and Discussion

MATLAB/SIMULINK is employed to implement the model of the proposed system of Fig. 1 and test the performance of the controllers. The overall model and control scheme have been

simulated for two diverse scenarios described in the following sub-sections. Parameter values used in the overall model are shown in Table 2, Table 3, Table 4, and Table 5.

For the two scenarios, we consider the following meteorological data:

- Insolation $G = 1000\ [W/m^2]$.
- Temperature $T = 293$ [K].

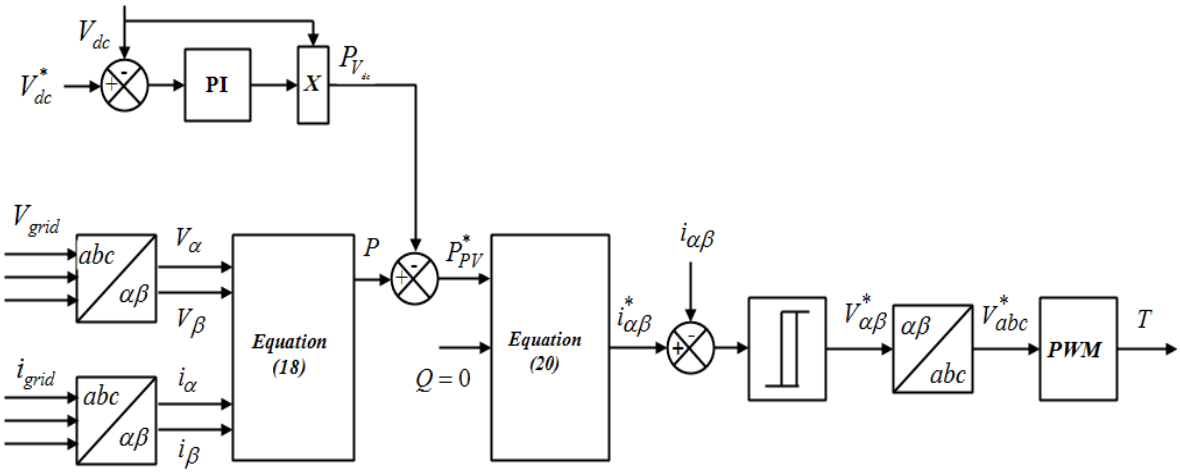

Fig. 7. Control block diagram of the injection process

Table 2. Parameters of the PV cell (Model KC200GT)

P_{PV}	W	200.143
$V_{oc,n}$	V	32.9
$I_{sc,n}$	A	8.21
$I_{0,n}$	A	$9.825.10^{-8}$
R_p	Ω	415.405
R_s	Ω	0.221
K_V	V/K	-0.123
K_I	A/K	0.0032
a	-	1.3
N_s	-	54
K	J/K	$1.381.10^{-23}$
q	C	$1.602.10^{-19}$

Table 3. DC/DC boost converter parameters

L_1	µH	11
C_B	mF	1

Table 4. Inverter parameters

V_{dc}	V	500
C	µF	2200

Table 5. Inductive filter value

L_f	mH	1

4.1. A Step-Change in Load

This scenario is assumed to simulate a variable load. The load is set to 5 kW initially. At $t = 0.5\ s$ it is suddenly changed to 7 kW and then decreased to 6 kW again at $t = 1\ s$. Fig. 8 shows the active power of the load, grid, and GPV. According to the meteorological data, the GPV generates constant power throughout this simulation. The grid must respond quickly to provide the difference between the power demanded by the load and that available in the PV system for the purpose of ensuring energy stability between the production system and the power demanded.

Fig. 9 (a), (b) and (c) show the waveforms of the load, grid and GPV currents, respectively. In these figures, it is noted that the waveforms of the currents are sinusoidal and that the frequency is maintained at 50 Hz.

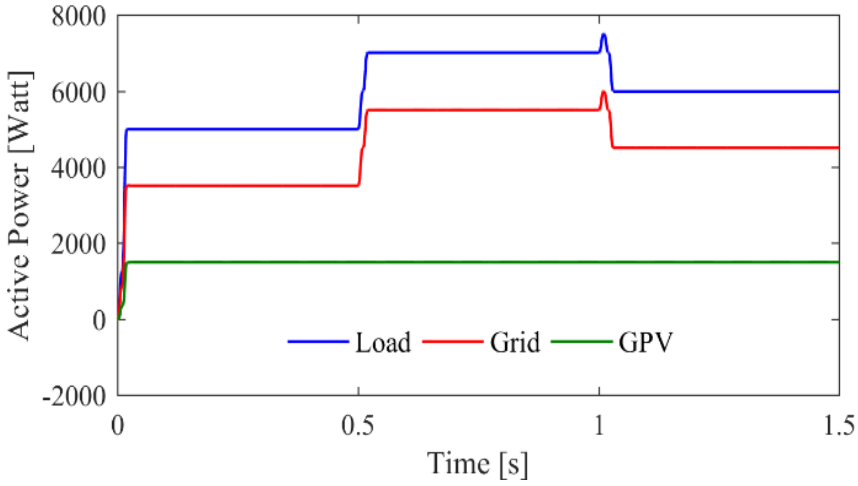

Fig. 8. Active power of the Load, Grid and GPV

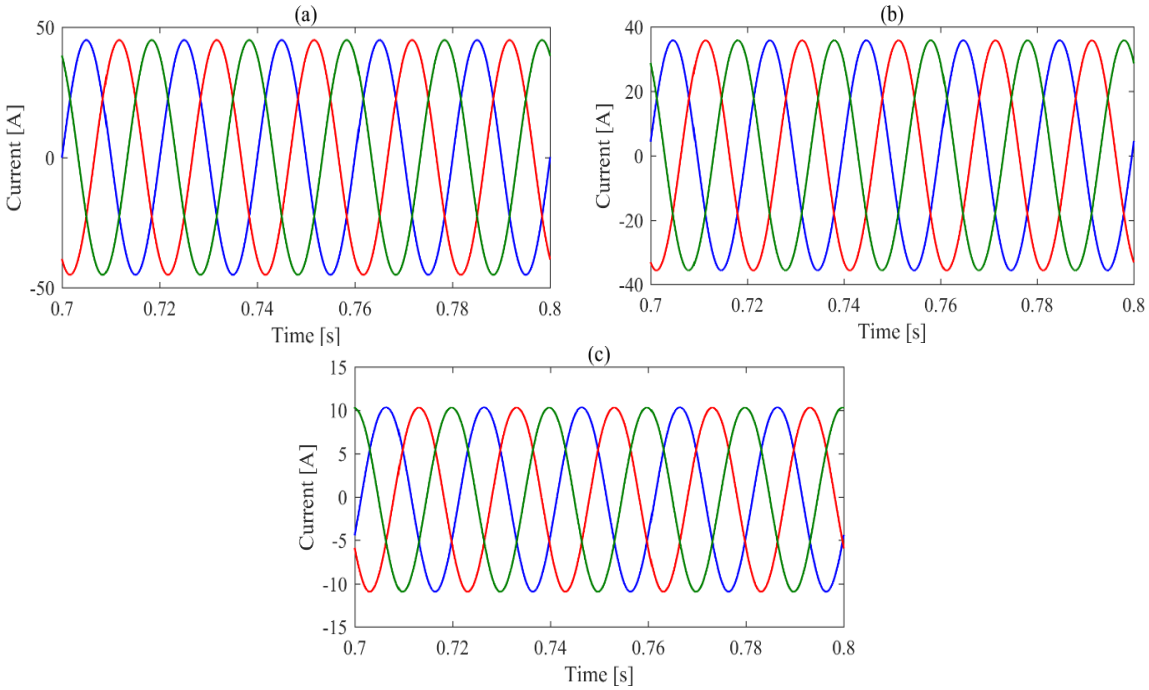

Fig. 9. Currents waveforms of Load, Grid and GPV

Fig. 10 shows the RMS current of load, grid and GPV. that are observed under simulated load variations. The direction of currents adopted in these simulations is based on the following equation:

$$i_{Load} = i_{Grid} + i_{PV} \tag{21}$$

Fig. 11 show the analysis of the THD of GPV current. We can clearly see that the THD for this current has a value of less than 5%. We conclude that integrating the inverter at three-levels improves the quality of energy produced by the PV system.

Fig. 12 shows the shape of the DC voltage. In order to better present the contribution of this article, we made a comparison between two PV systems with or without SMES to test the performance of balance and stability in the DC voltage. After this figure, it is clearly seen that the DC voltage follows its reference successfully. It is clear that the measured voltage follows its

reference successfully, it does not affect the variation of the load. But, with the use of SMES the stability of DC voltage is very efficient compared with a system without SMES.

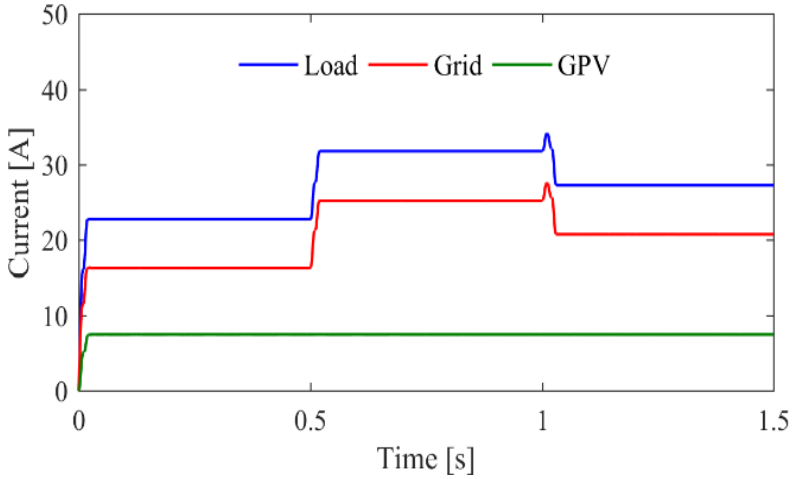

Fig. 10. RMS current of the Load, Grid and GPV

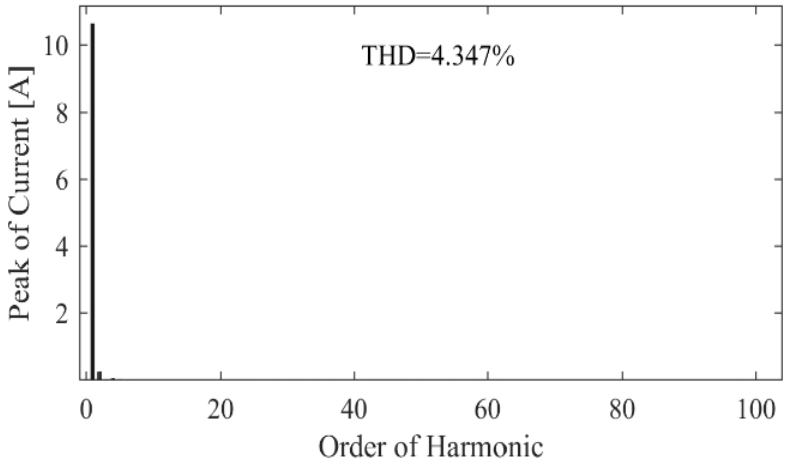

Fig. 11. THD of GPV current

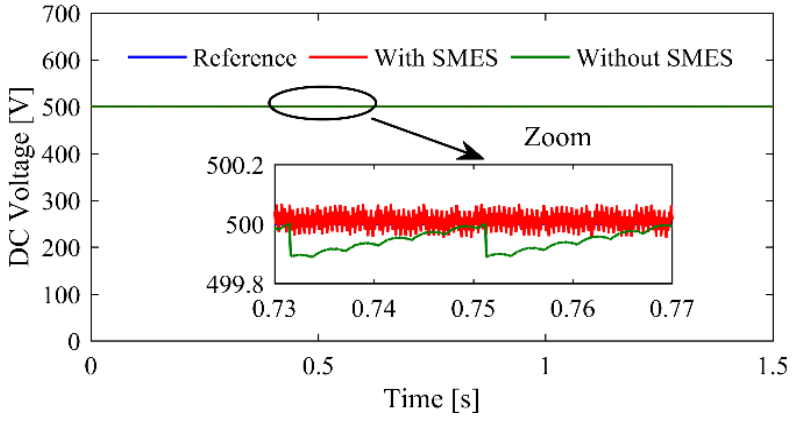

Fig. 12. DC voltage

Fig. 13 shows a duty cycle for the SMES. For this simulation test, we proposed that the SMES be fully loaded. During this simulation, it can be seen that the SMES is in discharge mode with a duty cycle which is less than 0.5. Fig. 14 shows the waveform of the voltage of the three-level inverter. We note that this voltage has the same image of the sinusoidal waveform and it has three voltage levels that indicate the uses of the three-level inverter.

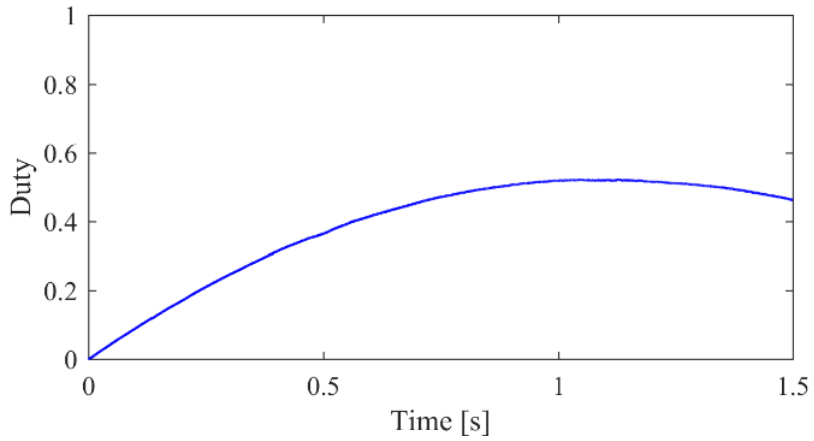

Fig. 13. Duty cycle

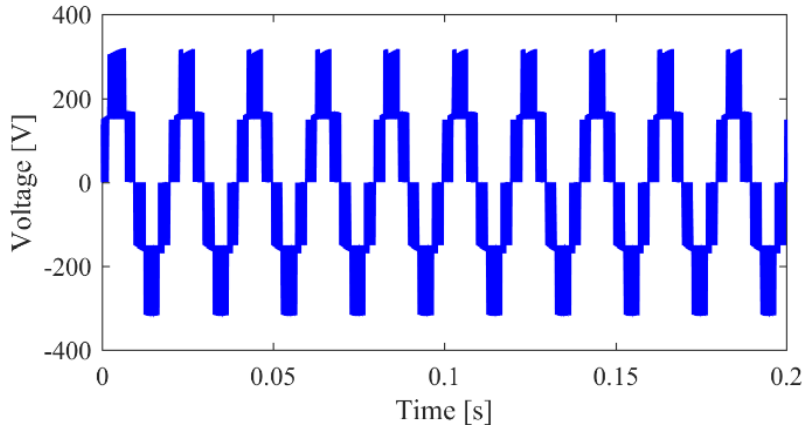

Fig. 14. Voltage of the three-level

4.2. Short Circuit of Three-Phase

This scenario is simulated with a Three-Phase Short-Circuit (TPSC) fault at $t = 0.78\,s$ and cleared $20\,ms$ later. Fig. 15 shows the grid and GPV output powers and the load demand. Clearly, the grid was able to balance the between the power required by the load and PV system. At $t = 0.78\,s$, when the TPSC is applied, the system exhibits a transient power unbalance. But, after the TPSC is cleared, the grid responds rapidly to provide the power demanded by the load. Fig. 16 shows the response of the DC voltage under this TPSC fault condition. With the SMES, the DC voltage has a superior performance as compared to the PV system without storage. This test confirms the importance of using the SMES in the PV system to ensure complete stability of the DC voltage.

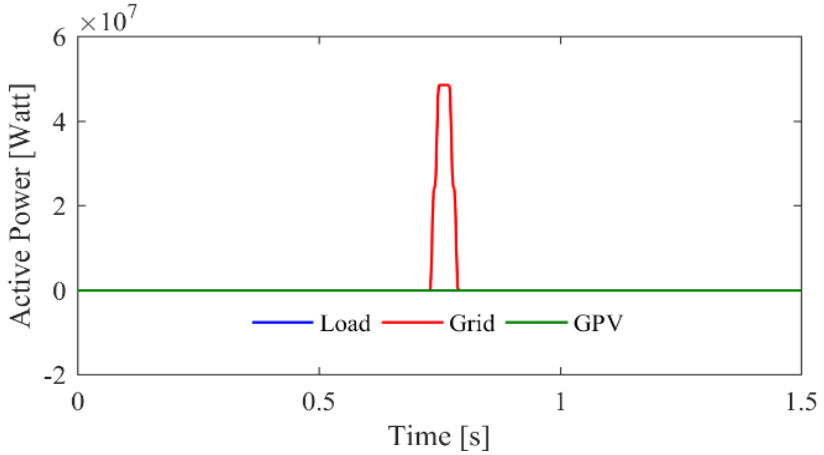

Fig. 15. Active power of the Load, Grid and GPV

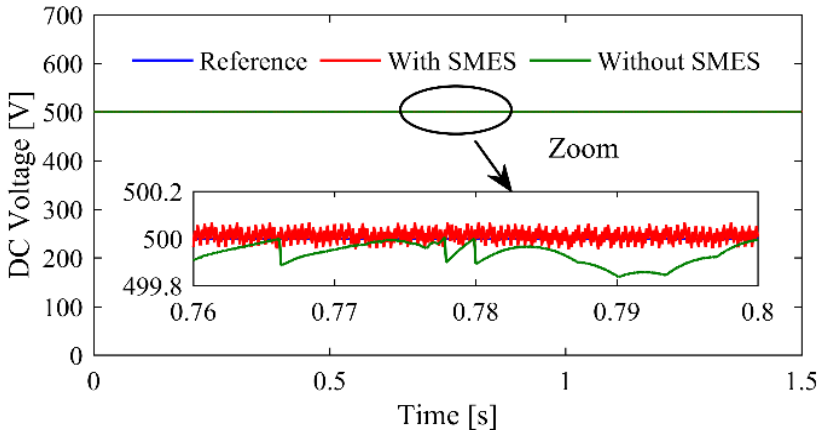

Fig. 16. DC voltage

5. Conclusions

The design and assessment of a control scheme for a hybrid (PV-SMES) system connected to the grid via a three-level NPC inverter is the main topic of this paper. The design of a clamping bridge control, the regulation of the DC voltage, and a storage system based on SMES to stabilize the DC bus voltage of the grid-connected PV system are some of the control strategies that have been suggested in this study to improve the system's performance. A number of simulation situations, such as load variation and TPSC failure, have been used to assess the suggested control strategy. The findings of a comparison simulation analysis between the suggested PV with and without SMES for DC voltage stability show that the SMES performs better. To further test the robustness of the system, future research could investigate the integration of additional energy storage systems or different failure circumstances. Further understanding of the control scheme's useful applications would also be possible by putting real-time experimental validation into practice and taking larger systems' scalability into account.

Author Contribution: All authors contributed equally to the main contributor to this paper. All authors read and approved the final paper.

Data Availability: The data used to support the findings of this study are available at reasonable request from the corresponding author.

Acknowledgements: The authors would like to acknowledge the financial support of Algeria's Ministry of Higher Education and Scientific Research. This work was supported by the L2GEGI laboratory at the University Ibn-Khaldun (Tiaret, Algeria) in collaboration with School of Engineering and Technology, University of Hertfordshire, Hatfield, UK.

Funding: The authors received no specific funding for this work.

Conflicts of Interest: The authors declare that they have no conflicts of interest.

Nomenclature

I_{ph}	Light-Generated Current
I_d	Current of the diode
I_p	Current flowing through the parallel resistor R_p
I_{PV}	Net current of the PV cell
V_{PV}	Cell voltage
V_d	Diode voltage
R_p, R_s	parallel and series resistances of the cell respectively
P_{PV}	Photovoltaic system output power
P_{Load}	Load power

L Inductor of DC-DC boost converter
C Capacitor of DC-DC boost converter
L_f Inductive filter
C_1, C_2 Capacitors of inverter
V_{dc} DC-link voltage
V_{dc}^* Reference of DC-link voltage.

References

[1] M. Awad *et al*., "A review of water electrolysis for green hydrogen generation considering PV/wind/hybrid/hydropower/geothermal/tidal and wave/biogas energy systems, economic analysis, and its application," *Alexandria Engineering Journal*, vol. 87, pp. 213–239, 2024, https://doi.org/10.1016/j.aej.2023.12.032.

[2] N. F. Ibrahim *et al*., "A new adaptive MPPT technique using an improved INC algorithm supported by fuzzy self-tuning controller for a grid-linked photovoltaic system," *PLoS One*, vol. 18, no. 11, pp. 1–22, 2023, https://doi.org/10.1371/journal.pone.0293613.

[3] P. Sinha *et al*., "Efficient automated detection of power quality disturbances using nonsubsampled contourlet transform & PCA-SVM," *Energy Exploration & Exploitation*, 2025, https://doi.org/10.1177/01445987241312755.

[4] V. Kumar *et al*., "A Novel Hybrid Harris Hawk Optimization – Sine Cosine Transmission Network," *Energies*, vol. 17, no. 19, p. 4985, 2024, https://doi.org/10.3390/en17194985.

[5] N. F. Ibrahim, A. Alkuhayli, A. Beroual, U. Khaled, and M. M. Mahmoud, "Enhancing the Functionality of a Grid-Connected Photovoltaic System in a Distant Egyptian Region Using an Optimized Dynamic Voltage Restorer : Application of Artificial Rabbits Optimization," *Sensors*, vol. 23, no. 16, p. 7146, 2023, https://doi.org/10.3390/s23167146.

[6] N. F. Ibrahim *et al*., "Operation of Grid-Connected PV System With ANN-Based MPPT and an Optimized LCL Filter Using GRG Algorithm for Enhanced Power Quality," *IEEE Access*, vol. 11, pp. 106859-106876, 2023, https://doi.org/10.1109/ACCESS.2023.3317980.

[7] T. Al Smadi, A. Handam, K. S. Gaeid, A. Al-Smadi, Y. Al-Husban, and A. smadi Khalid, "Artificial intelligent control of energy management PV system," *Results in Control and Optimization*, vol. 14, p. 100343, 2024, https://doi.org/10.1016/j.rico.2023.100343.

[8] H. M. I. Saleeb *et al*., "Highly Efficient Isolated Multiport Bidirectional DC/DC Converter for PV Applications," *IEEE Access*, vol. 12, pp. 114480-114494, 2024, https://doi.org/10.1109/ACCESS.2024.3442711.

[9] R. Kassem *et al*., "A Techno-Economic-Environmental Feasibility Study of Residential Solar Photovoltaic / Biomass Power Generation for Rural Electrification : A Real Case Study," *Sustainability*, vol. 16, no. 5, p. 2036, 2024, https://doi.org/10.3390/su16052036.

[10] D. P. Mishra, K. K. Rout, S. Mishra, M. Nivas, R. K. P. R. Naidu, and S. R. Salkuti, "Power quality enhancement of grid-connected PV system," *International Journal of Power Electronics and Drive Systems*, vol. 14, no. 1, pp. 369–377, 2023, http://doi.org/10.11591/ijpeds.v14.i1.pp369-377.

[11] T. Boutabba *et al*., "Design of a Small Wind Turbine Emulator for Testing Power Converters Using dSPACE 1104," *International Journal of Robotics and Control Systems*, vol. 5, no. 2, pp. 698–712, 2025, https://doi.org/10.31763/ijrcs.v5i2.1685.

[12] K. Himour, K. Ghedamsi, and E. M. Berkouk, "Supervision and control of grid connected PV-Storage systems with the five level diode clamped inverter," *Energy Conversion and Management*, vol. 77, pp. 98–107, 2014, https://doi.org/10.1016/j.enconman.2013.09.001.

[13] G. Tsengenes and G. Adamidis, "A multi-function grid connected PV system with three level NPC inverter and voltage oriented control," *Solar Energy*, vol. 85, no. 11, pp. 2595–2610, 2011, https://doi.org/10.1016/j.solener.2011.07.017.

[14] N. Altin and S. Ozdemir, "Three-phase three-level grid interactive inverter with fuzzy logic based maximum power point tracking controller," *Energy Conversion and Management*, vol. 69, pp. 17–26, 2013, https://doi.org/10.1016/j.enconman.2013.01.012.

[15] M. M. Mahmoud, "Improved current control loops in wind side converter with the support of wild horse optimizer for enhancing the dynamic performance of PMSG-based wind generation system," *International Journal of Modelling and Simulation*, vol. 43, no. 6, pp. 952–966, 2023, https://doi.org/10.1080/02286203.2022.2139128.

[16] S. Ashfaq *et al*., "Comparing the Role of Long Duration Energy Storage Technologies for Zero-Carbon Electricity Systems," *IEEE Access*, vol. 12, pp. 73169-73186, 2024, https://doi.org/10.1109/ACCESS.2024.3397918.

[17] I. E. Maysse *et al*., "Nonlinear Observer-Based Controller Design for VSC-Based HVDC Transmission Systems Under Uncertainties," *IEEE Access*, vol. 11, pp. 124014-124030, 2023, https://doi.org/10.1109/ACCESS.2023.3330440.

[18] B. Belabbas, M. Denai, and T. Allaoui, "Hierarchical energy management and control to improve the reliability and efficiency of wind farms connected to the grid," *International Transactions on Electrical Energy Systems*, vol. 30, no. 7, 2020, https://doi.org/10.1002/2050-7038.12400.

[19] F. Menzri, T. Boutabba, I. Benlaloui, H. Bawayan, M. I. Mosaad, and M. M. Mahmoud, "Applications of hybrid SMC and FLC for augmentation of MPPT method in a wind-PV-battery configuration," *Wind Engineering*, vol. 48, no. 6, pp. 1186-1202, 2024, https://doi.org/10.1177/0309524X241254364.

[20] A. Fatah *et al*., "Design, and dynamic evaluation of a novel photovoltaic pumping system emulation with DS1104 hardware setup: Towards innovative in green energy systems," *PLoS One*, vol. 19, no. 10, p. e0308212, 2024, https://doi.org/10.1371/journal.pone.0308212.

[21] F. Merahi and E. M. Berkouk, "Back-to-back five-level converters for wind energy conversion system with DC-bus imbalance minimization," *Renewable Energy*, vol. 60, pp. 137–149, 2013, https://doi.org/10.1016/j.renene.2013.05.001.

[22] B. Belabbas, T. Allaoui, M. Tadjine, and M. Denai, "Power Quality Enhancement in Hybrid Photovoltaic-Battery System based onthree-Level Inverter associated with DC bus Voltage Control," *Journal of Power Technologies*, vol. 97, no. 4, pp. 272–282, 2017, https://papers.itc.pw.edu.pl/index.php/JPT/article/view/992.

[23] S. J. Yaqoob, H. Arnoos, M. A. Qasim, E. B. Agyekum, A. Alzahrani, and S. Kamel, "An optimal energy management strategy for a photovoltaic/li-ion battery power system for DC microgrid application," *Frontiers in Energy Research*, vol. 10, 2023, https://doi.org/10.3389/fenrg.2022.1066231.

[24] A. Salvadori, D. Grazioli, and M. G. D. Geers, "Governing equations for a two-scale analysis of Li-ion battery cells," *International Journal of Solids and Structures*, vol. 59, pp. 90–109, 2015, https://doi.org/10.1016/j.ijsolstr.2015.01.014.

[25] P. Naderi and F. Fallahi, "A novel structure proposal for distributed generation using SMES and PV system with relative controllers design," *Energy Systems*, vol. 6, no. 2, pp. 153–172, 2015, https://doi.org/10.1007/s12667-014-0133-5.

[26] S. R. K. Joga et al., "Applications of tunable-Q factor wavelet transform and AdaBoost classier for identification of high impedance faults: Towards the reliability of electrical distribution systems," *Energy Exploration & Exploitation*, vol. 42, no. 6, pp. 2017-2055, 2024, https://doi.org/10.1177/01445987241260949.

[27] A. M. Ewias *et al*., "Advanced load frequency control of microgrid using a bat algorithm supported by a balloon effect identifier in the presence of photovoltaic power source," *PLoS One*, vol. 18, no. 10, 2023, https://doi.org/10.1371/journal.pone.0293246.

[28] A. Saxena, R. Kumar, M. Amir, and S. M. Muyeen, "Maximum power extraction from solar PV systems using intelligent based soft computing strategies: A critical review and comprehensive performance analysis," *Heliyon*, vol. 10, no. 2, p. e22417, 2024, https://doi.org/10.1016/j.heliyon.2023.e22417.

[29] N. Debdouche, B. Deffaf, H. Benbouhenni, Z. Laid, and M. I. Mosaad, "Direct Power Control for Three-Level Multifunctional Voltage Source Inverter of PV Systems Using a Simplified Super-Twisting Algorithm," *Energies*, vol. 16, no. 10, p. 4103, 2023, https://doi.org/10.3390/en16104103.

[30] A. A. Kulaksiz and R. Akkaya, "Training data optimization for ANNs using genetic algorithms to enhance MPPT efficiency of a stand-alone PV system," *Turkish Journal of Electrical Engineering and Computer Sciences*, vol. 20, no. 2, pp. 241–254, 2012, https://doi.org/10.3906/elk-1101-1051.

[31] O. M. Lamine *et al*., "A Combination of INC and Fuzzy Logic-Based Variable Step Size for Enhancing MPPT of PV Systems," *International Journal of Robotics and Control Systems*, vol. 4, no. 2, pp. 877–892, 2024, https://doi.org/10.31763/ijrcs.v4i2.1428.

[32] A. M *et al*., "Prediction of Optimum Operating Parameters to Enhance the Performance of PEMFC Using Machine Learning Algorithms," *Energy Exploration & Exploitation*, vol. 43, no. 2, pp. 676-698, 2024, https://doi.org/10.1177/01445987241290535.

[33] A. K. Sharma *et al*., "Role of Metaheuristic Approaches for Implementation of Integrated MPPT-PV Systems: A Comprehensive Study," *Mathematics*, vol. 11, no. 2, p. 269, 2023, https://doi.org/10.3390/math11020269.

[34] B. Krishna Ponukumati et al., "Evolving fault diagnosis scheme for unbalanced distribution network using fast normalized cross-correlation technique," *PLoS One*, vol. 19, no. 10, pp. 1–23, 2024, https://doi.org/10.1371/journal.pone.0305407.

[35] M. Safarishaal and M. Sarvi, "New hybrid maximum power point tracking methods for fuel cell using artificial intelligent," *AIP Advances*, vol. 13, no. 4, p. 045207, 2023, https://doi.org/10.1063/5.0144806.

[36] D. Naamane, Z. Laid, and M. Fateh, "Power Quality Improvement Based on Third-Order Sliding Mode Direct Power Control of Microgrid-Connected Photovoltaic System with Battery Storage and Nonlinear Load," *Iranian Journal of Science and Technology, Transactions of Electrical Engineering*, vol. 47, no. 4, pp. 1473–1490, 2023, https://doi.org/10.1007/s40998-023-00627-4.

[37] M. Elmorshedy, M. M. Amin, F. F. M. El-Sousy and O. A. Mohammed, "DC-Bus Voltage Control of MPPT-based Wind Generation System Using Hybrid BESS-SMES System for Pulse Loads in Ship Power Applications," *2021 IEEE Applied Power Electronics Conference and Exposition (APEC)*, pp. 76-82, 2021, https://doi.org/10.1109/APEC42165.2021.9487114.

[38] J. X. Jin *et al*., "A superconducting magnetic energy storage with dual functions of active filtering and power fluctuation suppression for photovoltaic microgrid," *Journal of Energy Storage*, vol. 38, p. 102508, 2021, https://doi.org/10.1016/j.est.2021.102508.

[39] L. Chen *et al*., "Optimization of SMES-Battery Hybrid Energy Storage System for Wind Power Smoothing," *2020 IEEE International Conference on Applied Superconductivity and Electromagnetic Devices (ASEMD)*, pp. 1-2, 2020, https://doi.org/10.1109/ASEMD49065.2020.9276307.

[40] G. Rajapakse, S. Jayasinghe and A. Fleming, "Power Management of an Oscillating Water Column Wave Energy Converter with Battery/Supercapacitor Hybrid Energy Storage," *2018 8th International Conference on Power and Energy Systems (ICPES)*, pp. 246-251, 2018, https://doi.org/10.1109/ICPESYS.2018.8626942.

[41] T. Rout, M. K. Maharana, A. Chowdhury and S. Samal, "A Comparative study of Stand-alone Photo-Voltaic System with Battery storage system and Battery Supercapacitor storage system," *2018 4th International Conference on Electrical Energy Systems (ICEES)*, pp. 77-81, 2018, https://doi.org/10.1109/ICEES.2018.8442346.

[42] P. Wongdet and B. Marungsri, "Hybrid Energy Storage System in Standalone DC Microgrid with Ramp Rate Limitation for Extending the Lifespan of Battery," *2018 International Electrical Engineering Congress (iEECON)*, pp. 1-4, 2018, https://doi.org/10.1109/IEECON.2018.8712174.

[43] T. F. Agajie *et al*., "Integration of Superconducting Magnetic Energy Storage for Fast-Response Storage in a Hybrid Solar PV-Biogas with Pumped-Hydro Energy Storage Power Plant," *Sustainability*, vol. 15, no. 13, p. 10736, 2023, https://doi.org/10.3390/su151310736.

[44] K. S. Garud, S. Jayaraj, and M. Y. Lee, "A review on modeling of solar photovoltaic systems using artificial neural networks, fuzzy logic, genetic algorithm and hybrid models," *International Journal of Energy Research*, vol. 45, no. 1. pp. 6–35, 2021, https://doi.org/10.1002/er.5608.

[45] N. F. Ibrahim *et al*., "Multiport Converter Utility Interface with a High-Frequency Link for Interfacing Clean Energy Sources (PV\Wind\Fuel Cell) and Battery to the Power System: Application of the HHA Algorithm," *Sustainability*, vol. 15, no. 18, p. 13716, 2023, https://doi.org/10.3390/su151813716.

[46] Z. Jin et al., "A portable, auxiliary photovoltaic power system for electric vehicles based on a foldable scissors mechanism," *Energy and Built Environment*, vol. 5, no. 1, pp. 81–96, 2024, https://doi.org/10.1016/j.enbenv.2022.08.002.

[47] K. Ullah, M. Ishaq, F. Tchier, H. Ahmad, and Z. Ahmad, "Fuzzy-based maximum power point tracking (MPPT) control system for photovoltaic power generation system," *Results in Engineering*, vol. 20, p. 101466, 2023, https://doi.org/10.1016/j.rineng.2023.101466.

[48] A. Mitra and D. Chatterjee, "Coordinated control of SMES and wind farm during fault in order to restrict rotor angle acceleration of power systems," *International Transactions on Electrical Energy Systems*, vol. 29, no. 3, 2019, https://doi.org/10.1002/etep.2747.

[49] M. Khaleel, Z. Yusupov, Y. Nassar, H. J. El-khozondar, A. Ahmed, and A. Alsharif, "Technical challenges and optimization of superconducting magnetic energy storage in electrical power systems," *e-Prime - Advances in Electrical Engineering, Electronics and Energy*, vol. 5, p. 100223, 2023, https://doi.org/10.1016/j.prime.2023.100223.

[50] L. Fu, Y. Chen, M. Zhang, X. Chen, and B. Shen, "Multifunctional Superconducting Magnetic Energy Compensation for the Traction Power System of High-Speed Maglevs," *Electronics*, vol. 13, no. 5, p. 979, 2024, https://doi.org/10.3390/electronics13050979.

[51] S. Sharouni and M. Hedayati, "Superconductor magnetic energy storage system usage for distributed generation: Active/reactive power and voltage controller design in connected and disconnected cases," *International Transactions on Electrical Energy Systems*, vol. 28, no. 5, 2018, https://doi.org/10.1002/etep.2531.

[52] J. D. Barros and J. F. Silva, "Optimal Predictive Control of Three-Phase NPC Multilevel Converter for Power Quality Applications," *IEEE Transactions on Industrial Electronics*, vol. 55, no. 10, pp. 3670-3681, 2008, https://doi.org/10.1109/TIE.2008.928156.

[53] S. Ali, A. Prado, and M. Pervaiz, "Hybrid Backstepping-Super Twisting Algorithm for Robust Speed Control of a Three-Phase Induction Motor," *Electronics*, vol. 12, no. 3, p. 681, 2023, https://doi.org/10.3390/electronics12030681.

[54] K. Rsetam, M. Al-Rawi, Z. Cao, A. Alsadoon, and L. Wang, "Model based smooth super-twisting control of cancer chemotherapy treatment," *Computers in Biology and Medicine*, vol. 169, p. 107957, 2024, https://doi.org/10.1016/j.compbiomed.2024.107957.

[55] S. Ozdemir, N. Altin, and I. Sefa, "Single stage three level grid interactive MPPT inverter for PV systems," *Energy Conversion and Management*, vol. 80, pp. 561–572, 2014, https://doi.org/10.1016/j.enconman.2014.01.048.

[56] J. J. Shieh, K. I. Hwu, and S. J. Chen, "Two Types of Asymmetric Switched-Capacitor Five-Level Single-Phase DC-AC Inverters for Renewable Energy Applications," *Energies*, vol. 17, no. 5, p. 983, 2024, https://doi.org/10.3390/en17050983.

[57] S. Nallusamy and D. K. Rukmani, "Design and simulation of Arduino Nano controlled DC-DC converters for low and medium power applications," *International Journal of Electrical and Computer Engineering (IJECE)*, vol. 13, no. 2, pp. 1400–1409, 2023, http://doi.org/10.11591/ijece.v13i2.pp1400-1409.

[58] K. Zhou, Z. Xu, Q. Guo, L. Luan and W. Hu, "The Coordination Control of SMES and PV in LVDC Distribution System," *IEEE Transactions on Applied Superconductivity*, vol. 31, no. 8, pp. 1-5, 2021, https://doi.org/10.1109/TASC.2021.3103723.

[59] J. Pahasa and I. Ngamroo, "Two-Stage Optimization Based On SOC Control of SMES Installed in Hybrid Wind/PV System for Stabilizing Voltage and Power Fluctuations," *IEEE Transactions on Applied Superconductivity*, vol. 31, no. 8, pp. 1-5, 2021, https://doi.org/10.1109/TASC.2021.3089119.

[60] B. Benbouya, "Dynamic Assessment and Control of a Dual Star Induction Machine State Dedicated to an Electric Vehicle Under Short- Circuit Defect," *International Journal of Robotics and Control Systems*, vol. 4, no. 4, pp. 1731–1745, 2024, https://doi.org/10.31763/ijrcs.v4i4.1557.